第 30 卷第 10 期 无 机 化 学 学 报 Vol.30 No.10
2014 年 10 月 CHINESE JOURNAL OF INORGANIC CHEMISTRY 2447-2452

等离子体辅助法合成 α-Si_3N_4/SiO_2 纳米梳

王秋实* 张 伟 张丽娜 吕 航 陆晓东 吴志颖
(渤海大学新能源学院,锦州 121013)

摘要: 晶体的 α-Si_3N_4 内核和非晶的 SiO_2 外壳组成的纳米梳通过简单的直流电弧方法合成。通过 X 射线衍射(XRD)、扫描电子显微术(SEM)、透射电子显微术(TEM)、傅里叶红外光谱(FTIR)等对纳米梳进行表征。纳米梳的光致发光谱展现了两个强的发光峰,分别在 450 和 511 nm。α-Si_3N_4/SiO_2 核壳结构纳米梳生长机制为等离子体辅助气–固生长机制。

关键词: 纳米结构; 氮化物; 电弧放电; 光致发光
中图分类号: O613.61 **文献标识码**: A **文章编号**: 1001-4861(2014)10-2447-06
DOI: 10.11862/CJIC.2014.184

Plasma-Assisted Synthesis of α-Si_3N_4/SiO_2 Core-Shell Nanocombs

WANG Qiu-Shi* ZHANG Wei ZHANG Li-Na LÜ Hang LU Xiao-Dong WU Zhi-Ying
(*College of New Energy, Bohai University, Jinzhou, Liaoning* 121013, *China*)

Abstract: Nanocombs composed of crystalline α-Si_3N_4 inner core and amorphous SiO_2 outer shell were synthesized by a simple one-step method of direct current arc discharge without the addition of any catalysts or templates. The morphology and structure of the nanocombs were characterized by XRD, SEM, EDS, TEM and FTIR. The photoluminescence (PL) spectrum of the nanocombs shows two strong emission peaks at about 450 nm and 511 nm. The growth mechanism of the α-Si_3N_4/SiO core-shell nanocombs can be considered as plasma-assisted vapor-solid mechanism.

Key words: nanostructure; nitrides; arc discharges; photoluminescence

0 Introduction

One-dimensional (1D) structures with nanometer diameters, such as nanotubes and nanowires, have been the focus of extensive research due to their potential applications as interconnects or functional components in nanoscale electronic, optoelectronic, and mechanical devices [1]. In such device structures, increasing the packing density or scaling-down the device for efficiency improving is facilitated by adopting a nanocable structure in which semiconductor nanowire cores are sheathed with insulator or semiconductor nanotube shells [2]. Until now, a great many 1D nanowires with coaxial structures have been reported. Thus, investigations have been devoted to the synthesis of coaxial core/shell structures of Si/SiO_2[3], SiC/SiO_2[4], Zn/ZnO[5], GaP/Ga_2O_3[6] and GaN/Ga_2O_3[7] systems, where oxide shells were formed by the oxidation of core materials. Among these reports, coating a silica shell on metallic [8], magnetic [9], or semiconducting cores has been most often discussed owing to its outstanding advantages

收稿日期:2014-03-27。收修改稿日期:2014-06-30。
国家自然科学基金(No.11304020);辽宁省教育厅科学技术研究项目(No.L2013427)资助。
*通讯联系人。E-mail:wang_jiu_jiu@foxmail.com Phone: +86-416-3400708. Fax: +86-416-3400708

such as easy control of the deposition, controllable porosity and optical transparency. Furthermore it is a low-cost material to tailor the surface properties while maintaining the physical integrity of the core. In addition, silica-coated nanostructures are very useful for biological applications because they allow surface conjugation with amines, thiols, and carboxyl groups, which in turn can be linked to biomolecules[10].

Si_3N_4 is a wide-band-gap (5.3 eV) semiconductor extensively used in the optical and electrical device industries [11]. Especially, its nanowire counterpart has recently attracted much attention because of their enhanced hardness associated with their unique optical and other mechanical properties as compared with coarse-grained Si_3N_4 ceramic materials[12-13]. Si_3N_4/SiO_2 nanocables, with crystalline Si_3N_4 core and amorphous SiO_2 shell, are ideal semiconductor-insulator hererostructures in the radial direction, thus exhibiting excellent properties of both Si_3N_4 nanowires and SiO_2 nanotubes as expected. Several research groups have synthesized Si_3N_4/SiO_2 core-shell nanostructure by different methods. For example, crystalline Si_3N_4/amorphous SiO_2 nanocables have been synthesized from silicon substrates using N_2 as working gas at 1 250 ℃ without any catalysts[14]. Well-aligned coaxial nanocables, composed of a crystalline α-Si_3N_4 inner core and amorphous SiO_2 outer shell, were prepared on silicon substrates by pyrolysis of a preceramic polymer (perhydropolysilazane) with iron as catalyst [15]. α-Si_3N_4/SiO_2 nanocables have been synthesized by the reaction of silicon dioxide nanoparticles with active carbon at 1 450 ℃ in flowing nitrogen atmosphere[16]. Si_3N_4/SiO_2 nanoparticles have been prepared via the Stöber process, using Si_3N_4 nanoparticles as the seeds [17]. These approaches, however, normally require complex procedures, substrates, and long reaction time, in some cases, sophisticated and expensive heating systems and significant amounts of energy are required to maintain the high temperature conditions for long periods of time. Therefore, in this paper, the authors report a new synthesis route for α-Si_3N_4/SiO_2 core-shell nanocombs using direct current (DC) arc discharge without metal catalysts. This high-efficiency synthesis method is characterised by much shorter reaction time as well as increased yield. The growth mechanism of α-Si_3N_4/SiO_2 core-shell nanocombs is also discussed.

1 Experimental

The synthesis was carried out in an improved DC arc discharge plasma setup[18]. A tungsten rod, with the purity higher than 99.99%, 4 mm in diameter and 15 cm in length, was used as the cathode. Si powder (particle size 74 μm (~200 mesh), purity: 99.95%, Sinopharm Chemical Reagent Co., Ltd.) and SiO_2 powder (particle size 74 μm (~200 mesh), purity: 99.99%, Sinopharm Chemical Reagent Co., Ltd.) were mixed with a molar ratio of 1:1 in a ball mill and pressed into columns as reactants. A column, 18 mm in diameter and 4 mm in height, was placed into a water-cooled graphite crucible which acts as the anode. The reaction chamber was first evacuated to less than 1 Pa and then filled with argon several times to remove residual air completely. Then the working gas (NH_3, purity: 99.999%) was introduced into the chamber until the inner pressure reached 30 kPa. As the DC arc discharge was ignited, the input current was maintained at 100 A and the voltage was a little higher than 20 V. The power supply was turned off 10 min later. After passivation in Ar for 6 h, high yield of the white powder samples was gathered at the surface of tungsten rod.

SEM images of the sample were taken on a HITACHI S-4800 microscope operated on 10 kV and equipped with an energy dispersive spectrometer (EDS). Structural analysis of the products was carried out by XRD on a D8 DISCOVER GADDS diffractometer operated at 40 kV and 100 mA with Cu $K\alpha_1$ radiation (λ=0.154 056 nm). Scanning rate is $0.02°\cdot s^{-1}$ in a 2θ range of 10° to 80°. The diffraction patterns were recorded on an image plate. The morphology of the nanocombs, as well as HRTEM images and the selected area electron diffraction (SAED) patterns, were obtained via a JEM-2100F transmission electron microscope using an accelerating voltage of 200 kV. The FTIR study was carried out on

a Nicolet Avatar 360 FTIR spectrometer with the prepared powders diluted in KBr pellets. The PL spectrum was measured with a JY-T800 Raman spectrometer (excited with a He-Cd line at 325 nm). All measurements were performed at room temperature.

2 Results and discussion

Fig.1a is a typical low-magnication SEM image of the product. A large number of comb-like nanostructures are observed. The most attention-getting feature of the nanostructures is that the branches grow unilaterally on one side of the stems to form a unique asymmetric nanocomb structure. The stems are typically several tens of microns in length. Fig.1b is a high-magnication SEM image of a typical nanocomb. It can be seen that the wire-shaped branches are nearly perpendicular to the stem. The branches are in narrow distributed size of 50~200 nm and distributed at one side of the stem. The chemical composition of the nanocombs is characterized by EDS. The results shown in Fig.1c indicate that the nanocomb consists of mainly Si, N and O. Fig.1d shows the XRD pattern of the nanocombs. All the diffraction peaks can be indexed to the hexagonal crystal lattice of α-Si_3N_4 with the space group $P3_1c$ (159) and the cell constants a=0.776 8 nm and c = 0.562 5 nm, which is in good agreement with the standard values for bulk α-Si_3N_4(PDF No. 83-0700, a= 0.776 5 nm, c =0.562 7 nm). Besides the α-Si_3N_4 phase, an unobvious broad hump at 17°~30° (2θ) is found in the XRD pattern, which could be assigned to amorphous SiO_2.

Fig.2a is a typical TEM image of the as-grown nanocomb structures, revealing that the periphery of nanocomb is very smooth and clean. The nanocomb is composed of a core and a shell forming the core-shell structure. The thickness of the shell is around 25 nm and the core is around 100 nm. The total diameter of the stem including the outer SiO_2 sheath is 150 nm. The shell thickness of branches is also about 25 nm, and the core thickness of branches is very thin, however, only 15~20 nm. Fig.2b is the HRTEM image of a representative juncture of the stem and the branches. The parallel lattice fringes can be clearly seen from stem to branch. It can be seen that the branches and stem are virtually one integrated mass. The lattice fringe spacing of 0.67 and 0.56 nm agree well with the (100) and (001) planes of bulk α-Si_3N_4 (PDF No. 83-0700). The branches are epitaxial grown on the stems and the stem grows along <100 > direction, while the branches grow along <001 >

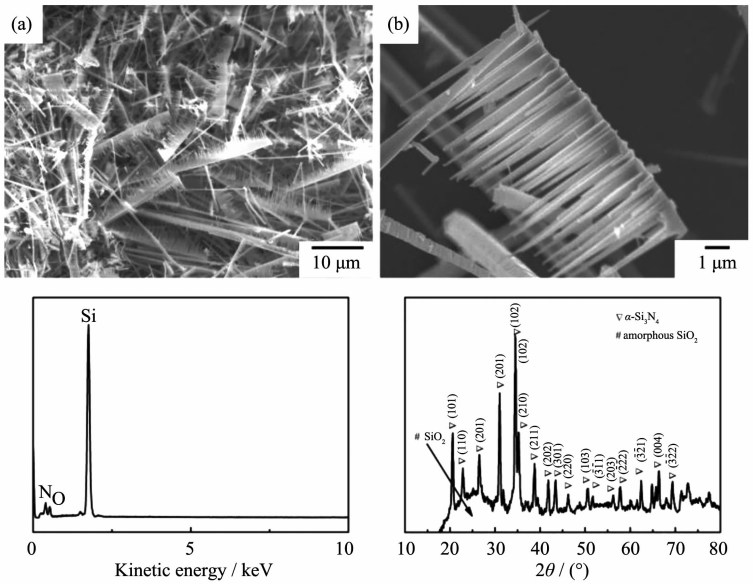

Fig.1 (a) Low-magnification and (b) high-magnification SEM images, (c) EDS spectrum obtained from the region marked with a rectangle in (b) and (d) XRD pattern of the α-Si_3N_4/SiO_2 core-shell nanocombs

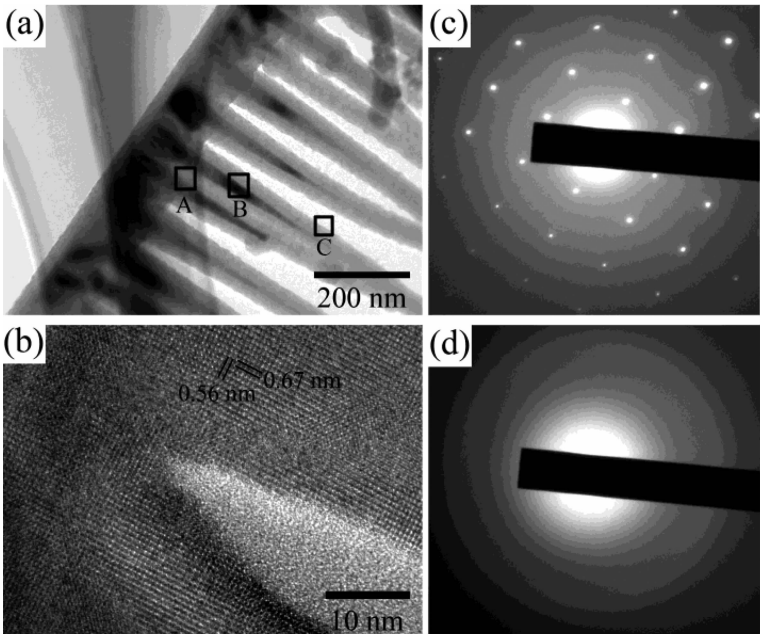

Fig.2 (a) TEM image of α-Si_3N_4/SiO_2 core-shell nanocomb; (b) HRTEM image for the selected area of A; (c) typical SAED pattern for the area of B and (d) typical SAED pattern for the area of C for the nanocomb in (a), respectively. Intentionally, area A is for interfacial juncture of nanocomb, area B is representative for the core of branch and area C for the shell of branch area.

direction. The SAED pattern recorded from the α-Si_3N_4 core (Fig.2c) and the SiO_2 shell (Fig.2d) is shown in the corresponding positions. The SAED from the core region of the nanocomb yields a set of diffraction spots of α-Si_3N_4 crystal and the shell region shows an amorphous ring pattern.

The FTIR spectrum of the product is shown in Fig.3. The FTIR absorption bands at 850, 684, 601 and 492 cm^{-1} correspond to the characteristic absorption bands of α-Si_3N_4 [19-20]. It confirms the presence of α-Si_3N_4 phase. The spectrum demonstrates

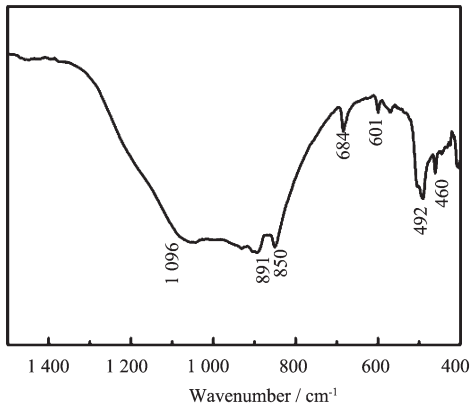

Fig.3 FTIR spectrum in the range of 1 400~400 cm^{-1} of the α-Si_3N_4/SiO_2 nanocombs

a wide absorption band in the range of 890~1 200 cm^{-1}. These are overlapped to the Si-N stretching vibration mode of α-Si_3N_4 and Si-O-Si stretching band [21-23]. The spectrum exhibit absorption peaks at 460 cm^{-1} corresponding to Si-O-Si rocking mode [24]. These results mean that the nanocombs are composed of closely α-Si_3N_4 and SiO_2.

Fig.4 shows photoluminescence spectrum of the α-Si_3N_4/SiO_2 nanocombs, which is excited by 325 nm UV light from He-Cd laser at room temperature. The α-Si_3N_4/SiO_2 nanocombs exhibit intensive luminescence. Previously, Robertsons [25] studies on Si_3N_4 show that there are four types of defects: Si-Si and N-N bonds, and Si and N dangling bonds. The Si-Si bond forms a bonding σ orbital and antibonding σ^* orbital that are separated by 4.6 eV in stoichiometric Si_3N_4. The silicon dangling bond forms a gap state about midgap, and the two nitrogen defect states that give rise to levels within the gap, namely, N_4^+ and N_2^0 are near the conduction and valence bands, respectively. The strong emission around 511 nm (2.4 eV) arises from recombination processes at the silicon dangling bond (4.6/2 ±0.1 =2.2 ~2.4 eV) [26-27]. The presence of SiO_2 shell will inevitably form Si-O-Si and

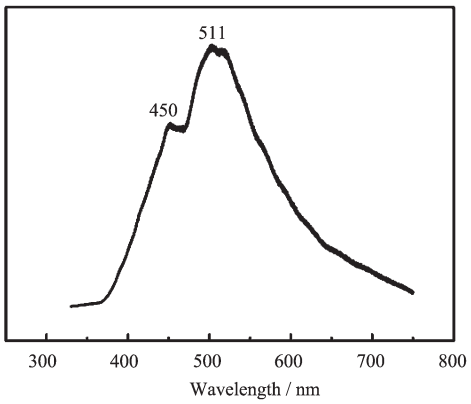

Fig.4　PL spectrum from the α-Si_3N_4/SiO_2 core-shell nanocombs

N-Si-O defective gap states, which leads to the emissions around 2.5 and 2.8 eV, respectively [28]. In this model, the PL peak at 450 nm is related to the incorporation of O during the synthesis of nanocombs, forming the Si-O-Si and N-Si-O defective gap states, which form the recombination between the intrinsic conduction band edge and Si dangling bonds. This peak is the same as the one in previous work on α-Si_3N_4/SiO_2 core-shell nanowires formed by CVD route (only one peak centered at 450 nm was observed) [22].

Several mechanisms have been proposed for the growth of α-Si_3N_4 nanowires, such as vapor-liquid-solid (VLS) [15], solid-liquid-gas-solid (SLGS) [29] and vapor-solid (VS) [22]. The VLS and SLGS mechanism seems not applicable in this case, because there are not any droplets observed on the ends of the stems and branches. Therefore, the growth mechanism of the α-Si_3N_4/SiO_2 nanocombs might well be a VS process, which can be described as follows.

As soon as the DC arc is ignited, the solid mixture of silicon and silica is evaporated drastically both thermally by the high temperature and by the bombardment of radicals of the arc zone. The following reactions can be expressed as follows:

$$Si(s)+SiO_2(s) \rightarrow SiO(g) \quad (1)$$

Due to the high temperature (above 1 500 ℃), the NH_3 will decompose to N_2 and H_2 vapors.

$$2NH_3(g) \rightarrow 3H_2(g)+N_2(g) \quad (2)$$

The SiO gases are diffused toward the cathode (tungsten rod) through an interfacial gas layer. They are adsorbed on the surface of the tungsten rod, where SiO would meet with the reactive radicals generated as a result of the excitation and ionization of flowing N_2 and H_2. These gaseous species then react with the nitrogenous radicals to form Si_3N_4 nanorods and H_2O via the following reaction.

$$3SiO(g)+2N_2(g)+3H_2(g) \rightarrow Si_3N_4(s)+3H_2O(g) \quad (3)$$

Firstly, the growth process is mainly a heterogeneous nucleation under low supersaturation condition, which leads to preferential growth along the <100> direction with a rapid rate to produce the central axial nanowires. Secondly, with SiO gas accumulated gradually and reaching a steady vapor pressure, the growth process changes from heterogeneous nucleation to homogeneous nucleation. Under this condition, the growth direction of α-Si_3N_4 then switches to <001>. During the formation of α-Si_3N_4 nanocomb, H_2O formed in reactions (3) reacts with the α-Si_3N_4 nanocomb to form solid SiO_2 which is located on their surface. The reaction can be expressed as follows[22].

$$Si_3N_4(s)+6H_2O(g) \rightarrow 3SiO_2(s)+4NH_3(g) \quad (4)$$

The addition of amorphous SiO_2 shell not only helps to produce straight stems and branches, but also blocks the growth along the cross section of the α-Si_3N_4 branches to form ultrathin central core. The whole growth process of the α-Si_3N_4/SiO_2 core-shell nanocomb is based on the VS growth mechanism.

3　Conclusions

In summary, we have synthesized α-Si_3N_4/SiO_2 core-shell nanocombs in large amounts via plasma-assisted the DC arc discharge method without any catalysts or templates. SEM and TEM morphologies show that the products usually have branches and stems, and branches grow unilaterally on one side of the stems to form a unique asymmetric nanocomb structure. XRD, FTIR, TEM and SAED results confirm that nanocombs are composed of a crystalline α-Si_3N_4 inner core and amorphous SiO_2 outer shell. Room-temperature PL spectrum of nanocombs shows broad visible emission around 400 ~700 nm, which can be attributed to defects in the Si_3N_4 and SiO_2

structure. The growth mechanism follows a plasma-assisted VS growing model.

References:

[1] Hill J P, Jin W S, Kosaka A, et al. *Science*, **2004**,**304**:1481-1483

[2] Lauhon L J, Gudiksen M S, Wang C L, et al. *Nature*, **2002**, **420**:57-61

[3] Cui L F, Ruffo R, Chan C K, et al. *Nano Lett*., **2009**,**9**:491-495

[4] Qiang X F, Li H J , Zhang Y L, et al. *J. Alloys Compd.*, **2013**,**572**:107-109

[5] Kong X Y, Ding Y, Wang Z L. *J. Phys. Chem. B*, **2004**,**108**: 570-574

[6] Liu B D, Bando Y, Tang C C, et al. *Appl. Phys. A*: *Mater. Sci. Process*., **2005**,**80**:1585-1588

[7] Lee S, Ham M H, Myoung J M, et al. *Acta Mater.*, **2010**,**58**: 4714-4722

[8] Sioss J A, Stoermer R L, Sha M Y, et al. *Langmuir*, **2007**,**23**: 11334-11341

[9] Zhang X F, Dong X L, Huang H, et al. *Acta Mater*., **2007**, **55**:3727-3733

[10]He J H , Zhang Y Y, Liu J, D. et al. *J. Phys. Chem. C*, **2007**, **111**:12152-12156

[11]Munakata F, Matsuo K, Furuya K, et al. *Appl. Phys. Lett.*, **1999**,**74**:3498-3500

[12]Zhang Y J, Wang N L, He R R, et al. *J. Cryst. Growth*, **2001**,**233**:803-808

[13]Yin L W, Bando Y, Zhu Y C, et al. *Appl. Phys. Lett*., **2003**, **83**:3584-3586

[14]Ran G Z, You L P, Dai L, et al. *Chem. Phys. Lett*., **2004**, **384**:94-97

[15]Fu X L, Peng Z J, Zhu N, et al. *Nanotechnology*, **2010**,**21**: 245603

[16]Wu X C, Song W H, Zhao B, et al. *Solid State Commun*., **2000**,**115**:683-686

[17]Qin J, Zhang P, Sun R, et al. *Electronic Materials and Packaging*, 2012 14th International Conference on Hong Kong: IEEE, **2012**:1-4

[18]WANG Feng (王峰), WANG Qiu-Shi(王秋实), CUI Qi-Liang(崔启良), et al. *Chinese J. Inorg. Chem.* (无机化学学报), **2009**,**25**:1026-1230

[19]Chaudhuri M G, Dey R, Mitra M K, et al. *Sci. Technol. Adv. Mater.*, **2008**,**9**:015002

[20]Zhu L L, Chen L Y , Huang T, et al. *J. Am. Ceram. Soc*., **2007**,**90**:1243-1245

[21]Ahmad M, Zhao J, Pan C F, et al. *J. Cryst. Growth*, **2009**, **311**:4486-4490

[22]Lin L W, He Y H. *CrystEngComm*, **2012**,**14**:3250-3256

[23]Wang F, Jin G Q, Guo X Y. *J. Phys. Chem. B*, **2006**,**110**: 14546-14549

[24]Yen H M, Jou S, Chu C J, et al. *Mater. Sci. Eng. B-Solid State Mater. Adv. Technol*., **2005**,**122**:240-245

[25]Robertson J Philos. *Mag. B-Phys. Condens. Matter Stat. Mech. Electron. Opt. Magn. Prop*., **1991**,**63**:47-77

[26]Zhang L G, Jin H, Yang W Y, et al. *Appl. Phys. Lett*., **2005**,**86**:061908

[27]Yang W, Zhang L, Xie Z, et al. *Appl. Phys. A*: *Mater. Sci. Process*., **2005**,**80**:1419-1423

[28]Liu Y Z, Zhou Y Q, Shi W Q, et al. *Mater. Lett*., **2004**,**58**: 2397-2400

[29]Yang W Y, Xie Z P, Li J J, et al. *J. Am. Ceram. Soc*. **2005**,**88**:1647-1650